Low-order finite elements for parameter identification in groundwater flow

Jiannan Xiang and Derek Elsworth

Pennsylvania State University, University Park, PA, USA

Improved evaluation and characterization of the geologic subsurface are necessary precursors to enhancing our ability to recover desirable resources and guard against undesirable contaminants. Mathematical models are increasingly used to assess the effects of these activities when the fidelity of material parameters describing the system control the reliability of the resulting prediction. Inverse models provide a formal means of space, or history, matching observed data to determine the unknown spatial distribution of the required parameters. The finite element method is one of the most popular numerical methods and is used in this study for transmissivity identification in steady groundwater flow. To optimize parameter identification, a comparison of different elements is carried out. It is well known that high-order elements usually result in improved accuracy in forward solution of engineering problems. However, this fact might not be true in the inverse solution. The study in this paper uses different element orders for Taylor's series analysis and in coding a finite element program. The analysis indicates that strong variation of transmissivity results in a larger residual error for high-order elements than for low-order elements. An example with an analytical solution is used for numerical comparison. The computed results show that low-order elements, rather than high-order elements, yield better results in parameter estimation. When the variation of unknown parameters is large, the error within the high-order elements is large. It is recommended that low-order finite elements or constant elements be used for an inverse solution. The comparison also illustrates that any minimization procedure may be used to minimize the residual error and to limit numerical difficulties in inverse solution. A two-dimensional example shows that the relative errors are very small when a constant element is used but that errors increase as the measured head distribution flattens.

Keywords: inverse solution, finite elements, groundwater

Introduction

Parameter identification is a very important activity in engineering fields when direct measurement is difficult or impossible. History matching of *in situ* observations, through use of numerical models, provides an important method for parameter estimation.

The finite element method has been an important numerical method in this area since the 1970s. Many kinds of finite elements are available for the solution of field problems. In most engineering fields in which the finite element method is used, high-order elements are usually favored, although they are more complex. First, they give a high solution accuracy. Second, they better simulate the variation of the unknown in each element. However, from the viewpoint of accuracy it is necessary to determine whether higher-order elements give better results in an inverse solution.

Considerable effort has been expended throughout the past two decades to develop and improve parameter estimation procedures.[1-5] Yeh[6] reports a comprehensive review of parameter identification procedures of groundwater hydrology. He examines the computational techniques that have been developed to solve the inverse problem and classifies them according to the error criterion used in the formulation. Frind and Pinder[7] applied a Galerkin finite element approach to an inhomogeneous isotropic aquifer for which steady-state piezometric head was known but transmissivity was unknown. To satisfy the uniqueness requirement, they used discharge magnitudes instead of transmissivity on the boundary (which may be difficult to obtain). Yeh, Yoon, and Lee[8] presented a new parameter identification method for a two-dimensional unsteady-state groundwater flow model. The accuracy of results depended on the representation of the finite elements. Weir[9] showed that in addition to ill-posedness the inverse problem may be undetermined if recharge is treated as a spatially and temporally variable distribution parameter. The consideration of generic errors showed that if the estimate for some derivative of head contains a significant error on one element for all time, then significant estimation errors are possible for all nodes and for all reservoir parameters. However, all these

studies ignored the element order, which may have a significant effect on the inverse solutions.

When the order of the finite element is low, the parameter identification problem becomes an over-determined problem. The solution may therefore exhibit improved accuracy. To prove this, elements with three different orders were used in the Taylor's series analysis and in coding a finite element program. Because many subroutines are available in the IBM Library,[10] it greatly simplified the complicated finite element solution. The analysis and computed results indicate that high-order finite elements cannot give high accuracy to the inverse solution, since implicit under-determination is included in the representation of the high-order element. The computed results also indicate that the direct inverse solution usually exhibits a large residual error caused by finite element discretization, especially when the differences between observations are very small in an element. The last squares procedure minimizes this error. To demonstrate the efficiency of constant elements in a two-dimensional problem, a two-dimensional groundwater flow system is used. The comparison shows that the computed results are quite close to the real values and that no numerical difficulty occurs during the computation, even though the head gradient in some areas is small.

The conclusions of this work may be applied to parameter identification and inverse problems in all engineering fields, although they were drawn specifically for a groundwater flow model. It is recommended that a constant element, rather than a high-order element, be used in parameter identification to ensure high quality in solution.

Governing differential equation

Basic assumptions for the one- or two-dimensional problems of groundwater flow considered in the following are that the aquifer is horizontal, inhomogeneous from point to point, and continuous in the region. Only confined problems are considered in which the transmissivity is directionally isotropic. Since the purpose of this paper is to find the best finite element for inverse solution, one may assume that all heads at mesh points are available so that the direct method of inverse solution can be used.

The governing equation for a groundwater flow system, under the above constraints can be written as

$$\frac{\partial}{\partial x_i}\left(T\frac{\partial h}{\partial x_i}\right) = \sum Q_w(t)\Pi\delta(x_i - x_{wi}) + S\frac{\partial h}{\partial t} \tag{1}$$

where i can be 1, 2, or 3 for one-, two-, or three-

dimensional cases, respectively, and the solution of a two-dimensional equation must satisfy the following conditions:

$$h(x, y, 0) = h_0(x_i) \qquad x_i \text{ in } R$$
$$h(x, y, t) = h_1(x_i, t) \qquad x_i \text{ in } dR_1$$
$$T\frac{\partial h}{\partial n} = h_{11}(x, t) \qquad x_i \text{ in } dR_{11}$$

where $h(x, y, t)$ is head at point (x, y);
$T(x, y)$ is transmissivity at (x, y);
S is the storage coefficient;
Q_w is the source-sink term;
x, y are coordinates in two-dimensional space;
t is time;
R is the flow region;
dR is the boundary of the aquifer $(dR_1 \cup dR_{11} = dR)$;
h_0, h_1, h_{11} are specified functions.
$\delta(x)$ is the Dirac delta function and $\delta(x) = \infty$ for $x = 0$; $\delta(x) = 0$ for $x \neq 0$;
x_{wi} are the coordinates of a well.

Inverse solution by the finite element method

Governing equation

Consider a steady problem (that is, the derivative $\partial h/\partial t = 0$ in equation (1)) where the piezometric heads are known at a finite number of points within the region R but the transmissivity $T(x, y)$ is unknown. The differential equation can be written as

$$\frac{\partial}{\partial x}\left[T(x, y)\frac{\partial h(x, y)}{\partial x}\right] + \frac{\partial}{\partial y}\left[T(x, y)\frac{\partial h(x, y)}{\partial y}\right]$$
$$= \sum_w Q_w\delta(x - x_w)\delta(y - y_w) \tag{2}$$

The boundary condition is

$$T(dR) = T_0 \tag{3}$$

or alternatively, using Frind and Pinder's[7] procedure,

$$T(dR) = \frac{-q_0}{\partial h/\partial n} \tag{4}$$

where q_0 is the discharge or recharge on the boundary. The transmissivity $T(x, y)$ can be expressed as

$$T(x, y) \approx \hat{T}(x, y) = \phi_i(x, y)T_i \tag{5}$$

where $\phi_i(x, y)$ is the shape function over the element with transmissivity $T(x, y)$ and T_i are the values at the nodes. Substituting equation (5) into equation (2) and integrating the whole equation on the region R with a weighting function ω_i, one has the following equation:

$$\int_R \left\{\frac{\partial}{\partial x}\left[\hat{T}(x, y)\frac{\partial h(x, y)}{\partial x}\right] + \frac{\partial}{\partial y}\left[\hat{T}(x, y)\frac{\partial h(x, y)}{\partial y}\right]\right\}\omega_i \, dR = \int_R \sum_w Q_w\delta(x - x_w)\delta(y - y_w)\omega_i \, dR \tag{6}$$

This equation can be integrated by applying Green's theorem to obtain

$$-\int_R \left[\hat{T}\frac{\partial h}{\partial x}\frac{\partial \omega_i}{\partial x} + \hat{T}\frac{\partial h}{\partial y}\frac{\partial \omega_i}{\partial y}\right] dR + \int_{R_{11}} \left[\omega_i\left(T\frac{\partial h}{\partial y}n_1 + T\frac{\partial h}{\partial y}n_2\right) dR_{11}\right] = \sum_w Q_w(x_w, y_w) \tag{7}$$

Since the flow boundary condition can be expressed as

$$T\frac{\partial h}{\partial y}n_1 + T\frac{\partial h}{\partial y}n_2 = h_{11} \tag{8}$$

where h_{11} is defined as before, equation (7) can be rewritten as

$$-\int_R \left[\hat{T}\frac{\partial h}{\partial x}\frac{\partial \omega_i}{\partial x} + \hat{T}\frac{\partial h}{\partial y}\frac{\partial \omega_i}{\partial y} \right] dR$$

$$+ \int_{R_{11}} \omega_i h_{11}\, dR_{11} = \sum_w Q_w(x_w, y_w) \tag{9}$$

The first derivative of head, h, is generally not available; therefore a shape function is chosen within the element that is continuously differentiable as Φ_k:

$$h(x, y) \approx \hat{h}(x, y) = \Phi_k h_k \tag{10}$$

where the function Φ_k is not necessarily identical to ϕ_i. A simple form for $\Phi_k(x, y)$ may be selected and, substituting equation (9) into (8), yields

$$\sum_c \int_{R^c} \left[\phi_j T_j \left[\frac{\partial}{\partial x}(\Phi_k h_k)\frac{\partial \omega_i}{\partial x} + \frac{\partial}{\partial y}(\Phi_k h_k)\frac{\partial \omega_i}{\partial y} \right] \right] dR^c$$

$$= -\sum_w Q_w(x_w, y_w) + \sum_c \int_{R_{11}} \omega_i h_{11}\, dR_{11}^c \tag{11}$$

where $i = 1, 2, 3, \ldots, n, j = 1, 2, 3, \ldots, m, k = 1, 2, 3, \ldots, n_c$, T_j comprises the transmissivity vector, and the total functional R and dR is replaced by $\sum R^c$ and $\sum dR^c$. In this, n is the number of nodes in the problem, n_c is number of elements in the problem, and m is number of nodes in an element. This equation can be written as

$$HT = Q_w + q \tag{12}$$

where Q_w is the inflow vector (from wells);
T is the transmissivity vector (unknown);
q is the outflow vector (on the boundary) and

$$q_i = \sum_c \int_{R_{11}} \omega_i h_{11}\, dR_{11}^c \tag{13}$$

H is the coefficient matrix

$$H_{i,j} = \sum_{k=1}^m h_k \int_{R^c} \left[\phi_j \left[\frac{\partial \Phi_k}{\partial x}\frac{\partial \omega_i}{\partial x} + \frac{\partial \Phi_k}{\partial y}\frac{\partial \omega_i}{\partial y} \right] \right] dR^c$$

$$i = 1, 2, 3, \ldots, n, \qquad j = 1, 2, 3, \ldots, n_c \tag{14}$$

where n and n_c are the numbers of nodes where head and transmissivity, respectively, are defined.

Element coefficient matrix

Coefficient matrices may be defined for elements of increasing functional variation. Using complementary terminology, these may be defined for constant, linear, and quadratic variations of the dependent variable.

Constant element

Consider the unknown parameter, transmissivity, as a constant in each element. For a two-node element with length $2L$, as shown in *Figure 1*,

$$T(x, y) = T_1 \tag{15}$$

$$\phi_j = 1 \tag{16}$$

The shape function Φ_k can be chosen as

$$\Phi_{i-1} = (1 - x/L)/2$$

$$\Phi_i = (1 + x/L)/2 \tag{17}$$

where the coordinate system is centered in the element.

Using weighting function $\omega_i = \Phi_i$ and substituting equation (16) into (14) yield the following element coefficient matrix $(2*1)$:

$$\mathbf{H}_c = \frac{h_{i-1} - h_i}{2L}\left\{ \begin{array}{c} 1 \\ -1 \end{array} \right\} \tag{18}$$

where h_{i-1} and h_i are heads at both ends of a pipe element, as shown in *Figure 1*.

Linear element

Assuming transmissivity to be linearly distributed in a two-node one-dimensional element of length $2L$, as shown in *Figure 2*, one obtains shape functions ϕ_i for transmissivity identical to those for heads. The same
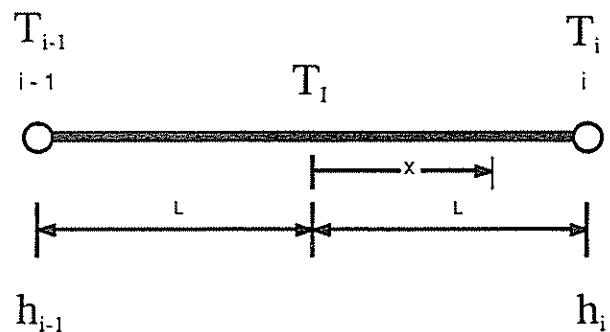

Figure 1. Schematic of nodes and coordinate configuration for a constant element
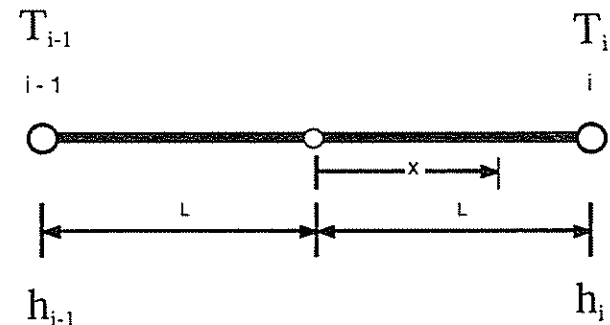

Figure 2. Schematic of nodes and coordinate configuration for a linear element

weighting function as equations (16) may be used, and the following equation is chosen:

$$\phi_i = \Phi_i = \omega_i \tag{19}$$

If we substitute equations (16) and (19) into (14), the element coefficient matrix is

$$\mathbf{H}_e = \frac{h_{i-1} - h_i}{4L} \begin{bmatrix} 1 & 1 \\ -1 & -1 \end{bmatrix} \tag{20}$$

where h_{i-1} and h_i have the same definition as above.

Quadratic element

The quadratic element may better represent the variation of transmissivity than a linear element when transmissivity is not linearly distributed over an element. For a three-node element of length $2L$, as shown in *Figure 3*, one can use the following shape functions:

$$\Phi_{i-1} = (x^2/L^2 - x/L)/2$$
$$\Phi_i = 1 - x^2/L^2 \tag{21}$$
$$\Phi_{i+1} = (x^2/L^2 + x/L)/2$$

If we use equations (19) and (21) and substitute into equation (14), the element coefficient matrix must have the following form:

$$\mathbf{H}_e = \begin{bmatrix} \dfrac{11C}{30} + \dfrac{\Delta h}{2} & \dfrac{4C}{15} + \dfrac{2\Delta h}{3} & \dfrac{C}{30} - \dfrac{\Delta h}{6} \\[2ex] -\dfrac{2C}{5} - \dfrac{2\Delta h}{3} & -\dfrac{8C}{15} & -\dfrac{2C}{5} + \dfrac{2\Delta h}{3} \\[2ex] \dfrac{C}{30} + \dfrac{\Delta h}{6} & \dfrac{4C}{15} - \dfrac{2\Delta h}{3} & \dfrac{11C}{30} - \dfrac{\Delta h}{2} \end{bmatrix} \tag{22}$$

where

$$C = (h_{i-1} - 2h_i + h_{i+1})/L$$
$$\Delta h = (h_{i-1} - h_{i+1})/2$$

h_{i-1} and h_{i+1} are the heads at both ends of a one-dimensional element, and h_i is the head at the midpoint.

Error analysis by Taylor's series

The rate of convergence of the solution within an element can be demonstrated through Taylor's series analysis. Since any element of dimension L with a complete solution expansion of order r can represent solution variations up to that order exactly in the forward solution, the local error in an arbitrary solution with a uniform mesh is estimated to be $O(L^{r+1})$, where $O(\ )$ represents the order of error. However, in the inverse solution, one may not obtain solution variations up to order r. To determine the accuracy of an inverse solution, it is necessary to determine the error expressions. Usually, there are two kinds of error. The first error is the residual error caused by discretizing differential equation using the finite element method. The second error is the error caused by measured error

or noise in observations. The following sections will determine the magnitudes of these two errors for different finite elements.

Residual error

The three elements discussed previously are evaluated for residual error. All analyses are based on a three-node line element. Comparison is made in parameters determined at the center node i, as shown in *Figure 4*, assuming that the values of h and T at the appropriate nodes are correct.

Error of constant element. Considering conservation of mass at node i and assuming that the residual error for equation (1) is Error$_1$, then from equation (18), one has (referring to *Figure 4*)

$$[-(h_{i-1} - h_i)T_I + (h_i - h_{i+1})T_{II}]/(2L)$$
$$= -q_i + \text{Error}_1 \tag{23}$$

T_I and T_{II} are the transmissivities of elements I and II, respectively. Using Taylor's series at the midpoints of elements I and II, one has

$$T_I = T_i - T_i' + T_i''/2 - T_i'''/6 + \ldots \tag{24}$$
$$T_{II} = T_i + T_i' + T_i''/2 + T_i'''/6 + \ldots \tag{25}$$

where primes denote successive orders of differentiation with respect to x as $T_i' = \partial T_i/\partial x$. Assuming that $q_i = 0$ and substituting equations (24) and (25) into
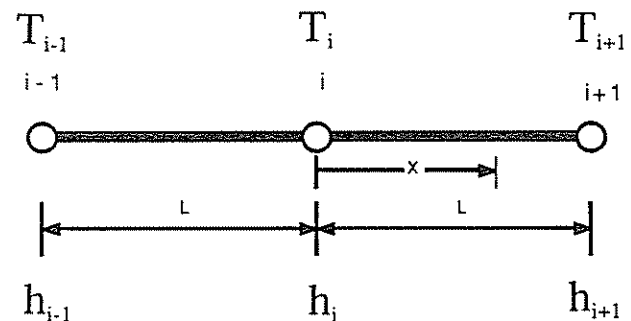

Figure 3. Schematic of nodes and coordinate configuration for a quadratic element
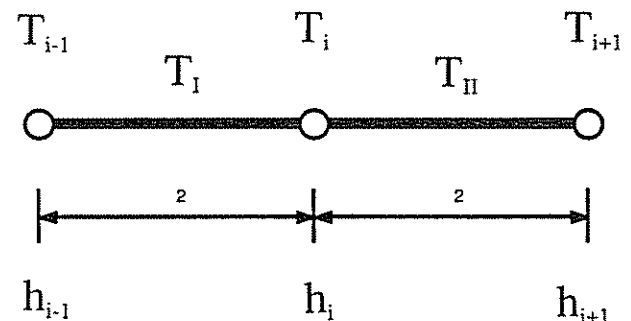

Figure 4. Schematic of nodes and coordinate configuration for a three-node pipe for error analysis

equation (23), one has

$$\text{Error}_1 = -DT_i/(2L) + \Delta h\, T_i' - DT_i''L/4$$
$$+ \Delta h\, T_i''L^2/6 + O(T_i^{IV}L^3) \quad (26)$$

where T_i^{IV} is the fourth derivative and $O(\ )$ denotes "error in order of."

According to *Figures 1* and *4*, and for $L = 1$, one has

$$\text{Error}_1 = -\frac{1}{2}DT_i + \Delta h\, T_i' - \frac{1}{4}DT_i''$$
$$+ \frac{1}{6}\Delta h\, T_i'' + O(T_i^{VI}) \quad (27)$$

where

$$\Delta h = (h_{i-1} - h_{i+1})/2$$

$$D = (h_{i-1} - 2h_i + h_{i+1})$$

Error of linear element. As is shown in *Figure 2*, at point i the continuity equation can be written as (from equation (20))

$$\text{Error}_2 = [(-h_{i-1} + h_i)T_{i-1} - DT_i$$
$$+ (h_i - h_{i+1})T_{i+1}]/(4L) + q_i \quad (28)$$

Using Taylor's series at nodes $i - 1$ and $i + 1$ in *Figure 4* yields

$$T_{i-1} = T_i - T_i'(2L) + T_i''(2L)^2/2$$
$$- T_i''(2L)^3/6 + O(T_i^{IV}(2L)^4) \quad (29)$$

$$T_{i+1} = T_i + T_i'(2L) + T_i''(2L)^2/2$$
$$+ T_i''(2L)^3/6 + O(T_i^{IV}(2L)^4) \quad (30)$$

Substituting equations (29) and (30) into (28) and assuming that $q_i = 0$ yields

$$\text{Error}_2 = -DT_i/(2L) + \Delta h\, T_i' - DT_i''L/2$$
$$+ 2L^2T_i''\Delta h + O(T_i^{IV}L^4) \quad (31)$$

for $L = 1$; then one has

$$\text{Error}_2 = -\frac{1}{2}DT_i + \Delta hT_i' - \frac{1}{2}DT_i''$$
$$+ \frac{2}{3}\Delta h\, T_i'' + O(T_i^{IV}) \quad (32)$$

Error of quadratic element. By using equation (22) and *Figures 3* and *4*, the following equation for residual error of the quadratic element may be determined from conservation of mass at node i:

$$\text{Error}_3 = [(-12A - 20\,\Delta h)T_{i-1} - 16AT_i$$
$$+ (-12A + 20\,\Delta h)T_{i+1}] - q_i \quad (33)$$

Substituting equations (29) and (30) into (33) for $q_i = 0$ yields

$$\text{Error}_3 = \frac{1}{30}\left[-40\,AT_i + 40\,\Delta h\, T_i'L - 12AT_i''L^2 \right.$$
$$\left. + \frac{20}{3}\Delta h\, T_i''L^3 + O(T_i^{IV}L^4) \right] \quad (34)$$

Since $A = D/L$,

$$\text{Error}_3 = -\frac{4}{3L}DT_i + \frac{4}{3}\Delta h\, T_i'L - \frac{2}{5}DT_i''L$$
$$+ \frac{2}{9}\Delta h\, T_i''L^2 + O(T_i^{IV}) \quad (35)$$

For the quadratic element, $L = 2$, and equation (35) may be defined as

$$\text{Error}_3 = -\frac{2}{3}DT_i + \frac{8}{3}\Delta h\, T_i' - \frac{4}{5}DT_i''$$
$$+ \frac{16}{9}\Delta h\, T_i'' + O(T_i^{IV}) \quad (36)$$

If we compare equations (27), (32), and (36), it is apparent that the residual error increases with the element order, from constant to quadratic. When the variation of T is very large or the high-order derivatives are not close to zero, the residual error will be extended, and high-order elements will not give a satisfactory solution. To demonstrate this more clearly, recall that the exact differential equation for the region $(i - 1, i + 1)$ in *Figure 4* is

$$\frac{\partial}{\partial x}\left(T\frac{\partial h}{\partial x}\right) = q = 0 \quad (37)$$

or

$$\frac{\partial T}{\partial x}\frac{\partial h}{\partial x} + T\frac{\partial^2 h}{\partial x^2} = 0 \quad (38)$$

By using finite differences the following approximate equation may be defined at node i (see *Figure 4*). For $L = 2$,

$$T_i(h_{i-1} - 2h_i + h_{i+1}) = -T_i'(h_{i-1} - h_{i+1}) \quad (39)$$

or

$$DT_i = -2\,\Delta h\, T_i' \quad (40)$$

Substituting equation (40) into equations (27), (32), and (36) yields respective appropriate error magnitudes of

$$\text{Error}_1 = \Delta h\, T_i' - \frac{1}{4}DT_i'' + \frac{1}{6}\Delta h\, T_i'' + O(T_i^{IV}L^3) \quad (41)$$

$$\text{Error}_2 = 2\,\Delta h\, T_i' - \frac{1}{2}DT_i'' + \frac{2}{3}\Delta h\, T_i'' + O(T_i^{IV}L^3) \quad (42)$$

$$\text{Error}_3 = 4\,\Delta h\, T_i' - \frac{4}{5}DT_i'' + \frac{16}{9}\Delta h\, T_i'' + O(T_i^{IV}L^3) \quad (43)$$

If we compare equations (41)–(43), it is apparent that each term in equation (41) is smaller than the corresponding terms in equations (42) and (43) with the exception of the first term in equation (41). Equations (41)–(43) show that each term representing residual error in the low-order element is smaller than that in successively higher-order elements. When the high-order derivatives are very small, the residual error in

the linear element is close to that of the constant element, but the residual error in the quadratic elements is double that in linear elements. When the high-order derivatives are large, the error in the high-order element is much larger. Although equation (40) is only an approximation of equation (35), it shows the parallel trend of error increase with order of element increase. Numerical results, to be documented later, corroborate this finding:

Measurement error

In general, the error caused by measurement can be expressed as

$$T^* = T + \epsilon_T \tag{44}$$

$$H^* = H + \epsilon_H \tag{45}$$

where T^* and H^* are respectively vectors and matrices of measured transmissivities and heads incorporating measurement errors ϵ_T and ϵ_H, respectively. In equation (45),

$$H = H(H) \quad \text{and} \quad \epsilon_H = H(\epsilon_h)$$

where ϵ_h is the measurement error vector.

If the error caused by head error is considered alone, then equation (12) can be written as

$$H^* T^* = Q \tag{46}$$

or

$$\epsilon_H T + H\epsilon_T + \epsilon_H \epsilon_T = 0 \tag{47}$$

Since the product vector $\epsilon_H \epsilon_T$ is very small, it may be considered to approach zero. The remaining error is therefore

$$\epsilon_T = -(H)^{-1}\epsilon_H T \tag{48}$$

This equation illustrates that the error in transmissivity depends on the error in head, matrix H, and vector T. Because the elements in H depend on the head difference in each finite element, ϵ_T will be very large when the head difference is very small. To determine these differences, the three elements evaluated in the preceding are considered to determine the influence of observation errors.

Constant element. Assuming the error in head distributions to be ϵ_h, the head vector incorporating mea-

surement noise can be expressed as $h^* = h + \epsilon_h$. The corresponding transmissivity vector T^* can be expressed as $T^* = T + \epsilon_T$, where ϵ_T is the parameter error caused by head observation errors. From equation (20), assuming that discharge remains constant along the element,

$$[(-h_{i-1} + h_i)T_1^* + (\epsilon_{h_{i-1}} + \epsilon_{h_i})T_1^*$$
$$+ (h_i - h_{i+1})T_{11}^* + (\epsilon_{h_i} - \epsilon_{h_{i+1}})T_{11}^*]\frac{1}{2L} = q \tag{49}$$

Ignoring the small, high-order errors leaves

$$[(-h_{i-1} + h_i)T_1 + (-h_{i-1} + h_i)\epsilon_{T_1}$$
$$+ (-\epsilon_{h_{i-1}} + \epsilon_{h_i})T_1 + (h_i - h_{i+1})T_{11}$$
$$+ (h_i - h_{i+1})\epsilon_{T_{11}} + (\epsilon_{h_i} - \epsilon_{h_{i+1}})T_{11}]\frac{1}{2L} = q_i \tag{50}$$

where ϵ_{h_i} is the head error at node i and ϵ_{T_1} is the transmissivity error in element 1.

If we use equation (23) for $q_i = 0$ and assume a zero residual error,

$$[(-h_{i-1} + h_i)\epsilon_{T_1} + (-\epsilon_{h_{i-1}} + \epsilon_{h_i})T_1$$
$$+ (h_i - h_{i+1})T_{11} + (h_i - h_{i+1})\epsilon_{T_{11}}$$
$$+ (\epsilon_{h_i} - \epsilon_{h_{i+1}})T_{11}]\frac{1}{2L} = 0 \tag{51}$$

or, gathering terms,

$$[(-h_{i-1} + h_i)\epsilon_{T_1} + (h_i - h_{i+1})\epsilon_{T_{11}}]$$
$$= -[(-\epsilon_{h_{i-1}} + \epsilon_{h_i})T_1 + (\epsilon_{h_i} - \epsilon_{h_{i+1}})T_{11}] \tag{52}$$

According to equations (40) and (41),

$$\frac{1}{2L}[(-h_{i-1} + h_i)\epsilon_{T_1} + (h_i - h_{i+1})\epsilon_{T_{11}}]$$
$$= \left[-D\epsilon_{T_i} - \frac{D}{4}\epsilon_{T_i}'' + \frac{\Delta h}{6}\epsilon_{T_i}'''\right] \tag{53}$$

If we ignore the high-order terms in equation (53), then equation (52) can be written as

$$-2D\epsilon_{T_i} = -[(-\epsilon_{h_{i-1}} + \epsilon_{h_i})T_1$$
$$+ (\epsilon_{h_i} - \epsilon_{h_{i+1}})T_{11}] + O(\epsilon_{Ti}'') \tag{54}$$

which may be expanded by Taylor's series with $L = 1$ to leave

$$\epsilon_{T_i} = \left[(-\epsilon_{h_{i-1}} + \epsilon_{h_i})\left(T_i - T_i' + \frac{1}{2}T_i'' - \frac{1}{6}T_i''' + \cdots\right) + (\epsilon_{h_i} - \epsilon_{h_{i+1}})\left(T_i + T_i' + \frac{1}{2}T_i'' + \frac{1}{6}T_i''' + \cdots\right)\right]\frac{1}{2D} + O(\epsilon_{T_i}'') \tag{55}$$

or, simplifying,

$$\epsilon_{T_i} = -\frac{\epsilon_D}{2D}T_i + \frac{\epsilon_{\Delta h}}{D}T_i' - \frac{1}{4D}\epsilon_D T_i'' + \frac{1}{6D}\epsilon_{\Delta h}T_i''' \tag{56a}$$

where

$$\epsilon_D = (\epsilon_{i-1} - 2\epsilon_i + \epsilon_{i+1})$$
$$\epsilon_{\Delta h} = (\epsilon_{i-1} - \epsilon_{i+1}) \tag{56b}$$

This represents the final description of error in evaluated transmissivity due to measurement errors.

Linear element. As a result of errors in head observations, the error in the resulting transmissivity determination may be evaluated from equation (29). Then, assuming that the residual error is zero,

$$[(-h_{i-1} + h_i)T^*_{i-1} + (\epsilon_{h_{i-1}} + \epsilon_{h_i})T^*_{i-1}$$
$$- DT^*_i - \epsilon_D T^*_i + (h_i - h_{i+1})T^*_{i+1}$$
$$+ (\epsilon_{h_i} - \epsilon_{h_{i+1}})T^*_{i+1}]\frac{1}{4L} = q_i \quad (57)$$

or using equation (28) for the zero residual error case enables equation (57) to be rewritten as

$$[(-h_{i-1} + h_i)\epsilon_{i-1} - D\epsilon_{T_{i-1}} + (h_i - h_{i+1})\epsilon_{i+1}$$
$$= (\epsilon_{h_{i-1}} + \epsilon_{h_i})T_{i-1} - \epsilon_D T_i + (\epsilon_{h_i} - \epsilon_{h_{i+1}})T_{i+1}]$$
$$\tag{58}$$

According to equation (32), if we use equation (40) and ignore the high-order terms of the error ϵ''_{T_i}, then

$$[(-h_{i-1} + h_i)\epsilon_{i-1} - D\epsilon_{T_{i-1}} + (h_i - h_{i+1})\epsilon_{i+1}$$
$$= -4DL\epsilon_{T_i} + O(\epsilon''_{T_i}) \tag{59}$$

Substituting equation (49) into equation (48) yields

$$\epsilon_{T_i} = [(-\epsilon_{h_{i-1}} + \epsilon_{h_i})T_{i-1} - \epsilon_D T_i$$
$$+ (\epsilon_{h_i} - \epsilon_{h_{i+1}})T_{i+1}]\frac{1}{4DL} + O(\epsilon''_{T_i}) \tag{60}$$

This may be expanded by Taylor's series for the terms T_{i-1} and T_{i+1} about T_i as given in equations (29) and (30) to yield

$$\epsilon_{T_i} = -\frac{\epsilon_D}{2DL}T_i + \frac{\epsilon_{\Delta h}}{D}T'_i - \frac{L}{2D}\epsilon_D T''_i$$
$$+ \frac{2L^2}{3D}\epsilon_{\Delta h}T'''_i + O(\epsilon''_{T_i}) \quad (61)$$

For the specific case of $L = 1$, equation (61) reduces to

$$\epsilon_{T_i} = -\frac{\epsilon_D}{2D}T_i + \frac{\epsilon_{\Delta h}}{D}T'_i - \frac{1}{2D}\epsilon_D T''_i$$
$$+ \frac{2}{3D}\epsilon_{\Delta h}T'''_i + O(\epsilon''_{T_i}) \quad (62)$$

to give the final error in transmissivity as a result of noise in the measurement of head.

Quadratic element. In a procedure similar to the previous, equation (33) can be rewritten as

$$[(-12A^* - 20\Delta h^*)T^*_{i-1} - 16AT^*_i$$
$$+ (-12A^* + 20\Delta h^*)T^*_{i+1}]/30 = -q_i \quad (63)$$

where $A^* = A + \epsilon_A$, $\Delta h^* = \Delta h + \epsilon_{\Delta h}$, and $\epsilon_A = \epsilon_{\Delta h}/L$. For $q_i = 0$ this equation can be reduced to

$$[(-12A - 20\Delta h)\epsilon_{T_{i-1}} - 16A\epsilon_{T_i} + (-12A + 20\Delta h)\epsilon_{T_{i+1}}]$$
$$= [(-12\epsilon_A - 20\epsilon_{\Delta h})T_{i-1} - 16\epsilon_A T_i + (-12\epsilon_A + 20\epsilon_{\Delta h})T_{i+1}] \tag{64}$$

According to equation (36), if we ignore high-order derivatives and use equation (40),

$$-2D\epsilon_{T_i} = -\frac{1}{30}[(-12\epsilon_A - 20\epsilon_{\Delta h})T_{i-1} - 16\epsilon_A T_i$$
$$+ (-12\epsilon_A + 20\epsilon_{\Delta h})T_{i+1}]$$
$$= \frac{4\epsilon_A}{3}T_i - \frac{4L}{3}\epsilon_{\Delta h}T'_i + \frac{2L^2}{5}\epsilon_A T''_i$$
$$- \frac{2L^3}{9D}\epsilon_{\Delta h}T'''_i + O(\epsilon''_{T_i}) \tag{65}$$

Since $\epsilon_A = \epsilon_D/L$ and from *Figure 4*, $L = 2$ for a quadratic element,

$$\epsilon_{T_i} = -\frac{\epsilon_D}{3D}T_i + \frac{4}{3D}\epsilon_{\Delta h}T'_i - \frac{2}{5D}\epsilon_D T''_i$$
$$+ \frac{8}{9D}\epsilon_{\Delta h}T'''_i + O(\epsilon''_{T_i}) \quad (66)$$

Equations (55), (62), and (66) representing transmissivity errors for the three element types indicate their complex dependence on head differentials, transmissivity constrasts, and derivatives of these constrasts. For a given error in head the resulting error in the higher-order element is always larger than that in the lower-order element. However, when transmissivity is constant, the error in the higher-order element

may be less. When high-order derivatives of transmissivity cannot be ignored, this error in the quadratic element is larger than that in both constant and linear elements.

Comparison of different finite elements

Minimization of residual error

As was mentioned above, in the inverse solution for transmissivity there are two types of errors. These are the computational error caused by noise in the measured head and the residual error resulting from discretizing a continuous equation by a piecewise approximation. For errors of the first type, time series data may be used to limit the solution error in transmissivity when the problem involves the nonsteady state.[11] In this problem, equation (12) with transient terms added for the unknown parameters may be solved directly, once the matrices $\mathbf{H}$, $\mathbf{Q}_w$, and q are assembled for all elements and the boundary condition of transmissivity is invoked.

For the latter case, residual errors exist in equation (11) and may be rewritten as

$$\mathbf{H}T - Q_w - q = \epsilon \tag{67}$$

and the least squares method is used to minimize the error. Solution requires that $\epsilon^T\epsilon$ is minimized such that

$\partial(\epsilon^T\epsilon)/\partial T = 0$ and simultaneously the second derivative defines a minimum. Solution for transmissivity by the method of least squares can be obtained from the preceding as

$$\mathbf{H}^T\mathbf{H}T = \mathbf{H}^T(Q_w + q) \qquad (68)$$

Since **H** is not a full-rank matrix, the transmissivity boundary condition has to be invoked. This procedure will require increased computational efforts but may give an improved solution. The following examples are developed to illustrate this.

Examples

Unidirectional flow in an inhomogeneous aquifer is used as an example. The width of the aquifer is uniform. Three cases are considered.

Case 1: Constant transmissivity. The constraints are

$$h_a = 0, \qquad h_b = 2.5$$
$$T_a = T_b = 1.0$$

The theoretical solution is

$$h = 0.4362182 \ln[(x + 1.34846923) * (-966.99896587/B)]$$
$$q_a = -0.481, \qquad q_b = 0.481$$
$$T = -0.05555556x^2 + 0.66666666x + 1$$

where h_a and h_b are the heads, T_a and T_b are transmissivities, q_a and q_b are discharges at both ends of the aquifer, x is the longitudinal coordinate, and $B = x - 13.34846923$.

Comparisons based on a one-dimensional example

Examples using the three finite element types were run both with and without the least squares procedure. All required heads are given using the above-mentioned analytical solutions. The Gauss-Newton method is used for inverse solution. For the constant element the least squares procedure (L.S.) had to be used, since the coefficient matrix **H** in equation (12) is not square (overdetermined). All computations were run on an IBM 3090. The sum of the square errors are shown in *Table 1*.

By comparing the results in *Table 1* it is apparent that the constant element gives the best results among the three elements and that the linear element has insufficient accuracy. The quadratic element gives the

The theoretical solution is

$$h = 0.41666667x$$
$$T = 1$$

Case 2: Linear transmissivity. The constraints are

$$h_a = 1.0, \qquad h_b = 3.0$$
$$q_a = 0.224, \qquad q_b = -0.224$$
$$T_a = 1, \qquad T_b = 2.0$$

The theoretical solution is

$$h = 2.8854 \ln(x/6 + 1) + 1$$
$$T = x/6 + 1$$

Case 3: Quadratic transmissivity. The constraints are

$$h_a = 2.0, \qquad h_b = 3$$
$$q_a = -0.35085, \qquad q_b = 0.35085$$
$$T_a = 1, \qquad T_b = 3$$

The theoretical solution is

largest error in all three cases. According to error expressions (41) and (42), for a constant element or linearly distributed transmissivity, the results obtained for the linear element and the constant element should be the same. However, the results in *Table 1* show the constant element to exhibit less error. In fact, the constant element performs better for a flatter head distribution when the Gauss-Elimination method is used. This is because the diagonal elements in Matrix **H** for linear, quadratic or higher-order elements depend on the second derivative of head. A flatter head distribution will result in small diagonal elements in the matrix **H**. This usually causes large numerical error. Conversely, the elements in matrix **H** for the constant element depend only on the gradient of head (or the first derivative). In this example, the minimum second derivative value is 0.02 and the minimum first derivative value is 0.24, resulting in differences in the inverse solutions. This confirms that the high-order element cannot give reasonable results for parameter identification. In fact, an implicit underdetermination

Table 1. The sum of squares errors for different cases and elements

Transmissivity	Constant element With L.S.	Linear element		Quadratic element	
		No L.S.	With L.S.	No L.S.	With L.S.
Constant	0.1×10^{-11}	0.33332	7.4×10^{-11}	1.0203	5.9×10^{-11}
Linear	7.19×10^{-7}	8.45×10^{-5}	8.43×10^{-5}	1.261×10^{-2}	1.243×10^{-2}
Quadratic	1.31×10^{-3}	1.75×10^{-2}	1.49×10^{-2}	5.045	0.216

exists in high-order elements, since the parameter can have a nonlinear variation.

It is apparent that the diagonal terms in the element matrix approach zero for linear and quadratic elements when hydraulic head is linearly distributed as shown in equations (18) and (20). This case promotes considerable numerical difficulties and may result in large errors. The values of *Table 1* without the least squares procedure and for constant transmissivity illustrate this point. In this instance the least squares procedure must be used to avoid serious error. The values of *Table 1* obtained by the least squares procedure indicate that the solutions were greatly improved. Other values of *Table 1* also show that the least squares procedure yields improved solutions, although it requires more CPU time to evaluate the matrix computations.

Two-dimensional example

As was mentioned above, the constant element yields the best solution among the three elements. This statement is true not only for one-dimensional problems, but also for two- or three-dimensional problems. To demonstrate the efficiency of constant elements, a two-

dimensional groundwater flow system is used that is similar in geometry to that of Carrera and Neuman[2] except that no areal recharge is accommodated. The aquifer configuration, the boundaries, and the transmissivity value for each zone are illustrated in *Figures 5(a)* and *5(b)*, where all recharge is defined in cubic meters per day. The boundaries are considered to be impermeable except for the inflow and constant head boundaries. No pumping well is considered.

A 6 × 6 mesh is used to obtain the head distribution. In the inverse solution, only a 3 × 3 mesh is used. A four-node constant element is used for the finite element solution in both forward and inverse modes. The resulting distribution of heads is shown in *Figure 6*. According to this distribution and the applied boundary conditions, the inverted parameters are obtained by using the least squares method and the Gauss method. The value of transmissivity in each zone and error percentages between the real and inverted transmissivities are shown in *Table 2*. The total square error is 85.72 m²/day², and the standard deviation is 4.14 m²/day² for all computed zones. *Table 2* also shows that the relative errors in zones 4 and 7 are very small and that the errors in zones 6 and 9 are larger. From *Figure 6* it is apparent that the variation of head gradients ($\partial^2 h/\partial x^2$)
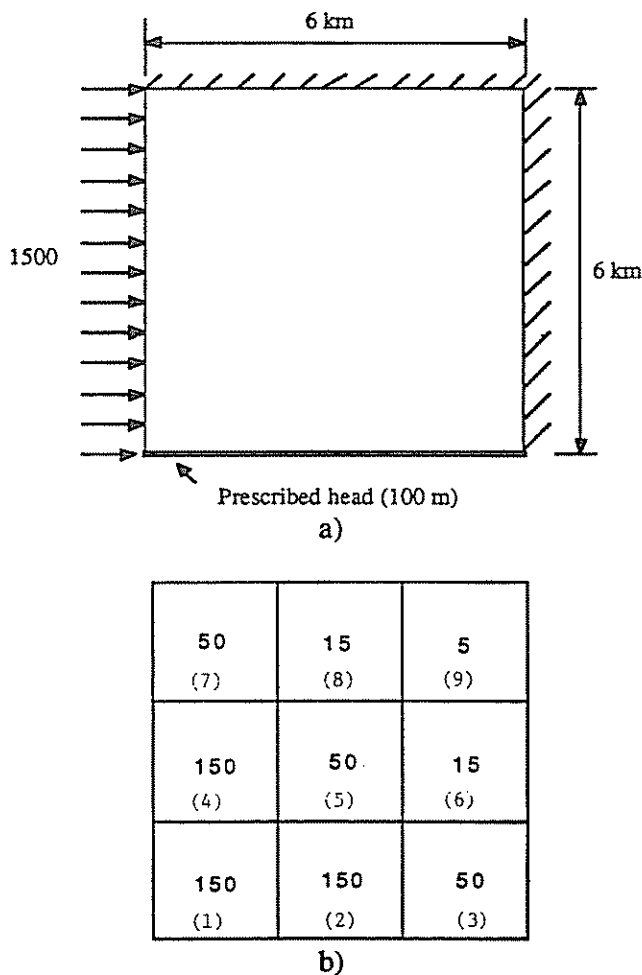

Figure 5. Aquifer configuration. (a) Boundary conditions (inflow rate in m³/day). (b) Transmissivity values for each zone
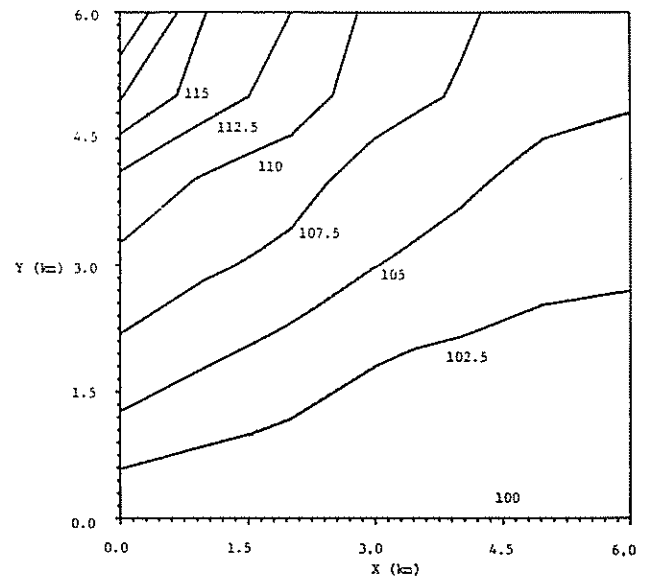

Figure 6. Distribution of heads for the two-dimensional example (with a 6 × 6 mesh)

Table 2. The computed transmissivity distribution and relative error in each zone

Zone number	Real value	Computed value	Relative error (%)
4	150	153.1345	2.09
5	50	56.1199	12.24
6	15	11.1096	−25.94
7	50	47.1944	−5.61
8	15	11.2757	−24.83
9	5	3.7493	−25.01

in those zones is correspondingly very small. The reason for this correspondence between increasing error magnitude and decreasing gradient is apparent in equation (56). For a given head distribution the error of the estimated parameter for lower values of the second derivative of measured head ($\partial^2 h/\partial x^2$) should be larger. In addition, if linear elements or quadratic elements are used, the estimation of transmissivity will be exacerbated because this error may be increased and the equations may become singular (owing to small diagonal elements in matrix H). However, if constant elements are used, no such difficulty occurs.

Conclusions

A study of parameter identification in groundwater flow systems was conducted. To determine the effects of different finite elements on the fidelity of parameter identification, three different finite elements were analyzed by using Taylor's series expansions. Examples were computed by the finite element method both with and without using the least squares procedure. The results illustrate the following:

1. In a numerical solution of the inverse problem the errors of estimated parameters result from both the residual error caused by discretization by the finite element method and from errors in observation (noise).
2. The residual error in transmissivity depends on both the absolute magnitude of transmissivity and the higher-order derivatives of this distribution. A strong variation of transmissivity will result in a large error in parameter estimates.
3. Low-order elements, rather than high-order elements, give the best accuracy for the inverse solution, according to the Taylor's series analyses and the results obtained by different elements. The constant element performs best among the three elements.
4. When observations of heads are linearly distributed over the field, linear or quadratic elements may cause some numerical difficulty as a result of singular coefficient matrices. This requires implementation of a special minimization procedure to overcome the problem.
5. The least squares procedure is very important to reduce the residual error and limit numerical difficulties for a direct solution.
6. A two-dimensional example shows that constant elements may also be applied to realistic problems for parameter estimation and yield high accuracy.

Acknowledgments

Nomenclature

h, h_k	Head and head at node k
h_a, h_b	Heads at both ends of aquifer in example problems
h_0, h_1, h_{11}	Specified function
H	Vector of head
$\mathbf{H}$	Matrix representing the distribution hydraulic head difference within the domain
L	Length of element
n, n_c	Numbers of nodes and elements
q_a, q_b	Recharge at both ends of the aquifer in example problems
T, T_0	Transmissivity and transmissivity on boundary
T_1, T_{11}	Transmissivity of element I, II
T_{i-1}, T_i, T_{i+1}	Transmissivity of node $i - 1$, i, $i + 1$
T_i^{IV}	Fourth derivative of transmissivity to coordinate direction
T^*	Transmissivity vector with noise
$\mathbf{T}$	Matrix representing the geometric transmissivity of the domain
T	Vector of transmissivity for the steady state
q_0	Recharge on the boundary
q	Recharge vector
Q_w	Discharge vector of wells
Q	Discharge and recharge vector
x, y, x_w, y_w	Coordinates and coordinates at wells
R	Flow region
dR	Boundary of the aquifer
dR_1, dR_{11}	Specified head boundary and discharge prescribed boundary, respectively
ϵ_{h_i}, ϵ_{T_i}	Error of head, error of transmissivity at node i
ϵ_h, ϵ_T	Error of vector head and transmissivity, respectively
ϵ_H	Error Matrix
ϵ	Error vector
ϕ_i, Φ_i	Shape functions
ω_i	Weighting function

References

1 Aral, M. Optimization approach to the identification of aquifer parameters in multilayer systems. *Fourth International Conference on Finite Elements in Water Resources*, Lisbon, Portugal, June 1986

2 Carrera, J. and Neuman, S. Estimation of aquifer parameters under transient and steady state conditions. 1: Maximum likelihood method incorporating prior information. *Water Resour. Res.* 1986, 22(2), 199–210

3 Dagan, G. and Rubin, Y. Stochastic identification of recharge, transmissivity, and storativity in aquifer transient flow: A quasi-steady approach. *Water Resour. Res.* 1988, 24(10), 1698–1710

4 Kuiper, L. A comparison of several methods for the solution of the inverse problem in two-dimensional steady state groundwater flow modeling. *Water Resour. Res.* 1986, 22(5), 705–714

5 Neuman, S. Calibration of distributed parameter groundwater flow models viewed as a multiple-objective decision process under uncertainty. *Water Resour. Res.* 1973, 22(4), 1006–1021

6 Yeh, W. Review of parameter identification procedures in

groundwater hydrology: The inverse problem. *Water Resour. Res.* 1986, **22**(2), 95–108

7   Frind, E. and Pinder, G. Galerkin solution of the inverse problem for aquifer transmissivity. *Water Resour. Res.* 1973, **9**(5), 1397–1410

8   Yeh, W., Yoon, Y. and Lee, K. Aquifer parameter identification with kriging and optimum parametrization. *Water Resour. Res.* 1983, **19**(1), 225–233

9   Weir, G. The direct inverse problem in aquifers. *Water Resour. Res.* 1989, **25**(4), 749–753

10   IBM, Engineering and Scientific Subroutine Library, *Guide and Reference, Release 3*, 4th ed., Nov. 1988

11   Xiang, J. and Elsworth, D. Parameter identification of non-steady groundwater flow systems. *Water Resour. Res.* (submitted for publication)